Synthesis and Characterization of Polyethylene Oxide and Nylon-6 Copolymer in a Fiber Form

Syang-Peng Rwei,[1] Yu-Chi Tseng,[1,2] Wei-Peng Lin[1,2]

[1]*Institute of Organic and Polymeric Materials, National Taipei University of Technology, Taipei, Taiwan, Republic of China*
[2]*Department of Raw Material and Yarns, Taiwan Textile Research Institute, New Taipei City 23674, Taiwan, Republic of China*

Received 6 July 2011; accepted 5 December 2011
DOI 10.1002/app.36676
Published online in Wiley Online Library (wileyonlinelibrary.com).

ABSTRACT: A series of poly(ethylene oxide) (PEO) and nylon-6 copolymers were synthesized through condensation reactions. The rheology of the prepared copolymers was tested using a capillary flow rheometer. The molar mass was investigated by performing basic analyses such as relative viscosity, gel permeation chromatograph, and amino-end group analysis. Their thermal properties were examined by differential scanning calorimetry, and the crystalline structure was determined using wide-angle X-ray diffraction. The results obtained from partially oriented yarn indicated a dramatically conversion from the γ form to the α form. Following the draw texture process, the α form dominated all draw textured yarn. Once the segments of PEO were introduced into the nylon-6 backbone, the moisture regain and q_{max} (warm/cool feeling) of the fabrics was enhanced remarkably. The surface resistivity of fabrics improved with increasing PEO content, which is mainly due to water absorption. © 2012 Wiley Periodicals, Inc. J Appl Polym Sci 000: 000–000, 2012

Key words: polyethylene oxide; nylon-6; crystallinity; fabric

INTRODUCTION

Nylon-6 fiber was first formed from a synthetic resin since 1940, and its use has continuously increased until now. The hydrogen bond that is formed by the amide repeat unit linkage in the backbone contributes substantially to its durability, toughness, high strength, and abrasion resistance. Meanwhile, the linear aliphatic structure makes it light, flexible, and soft. Nylon-6 polymer is converted to fibers through melt-spinning process. The characteristics of the fiber can be designed to satisfy a variety of specific requirements by adjusting the spinning or texturing process. Nylon-6 fiber absorbs less moisture than nature fibers. It makes the skin feel sticky and uncomfortable under certain circumstances. Like most of synthetic polymers, nylon-6 is an insulator and the fabric exhibits high electrical resistivity, which limits its range of applications. The literature includes several approaches for increasing the electrostatic dissipative of nylon.[1–3] One of the most important methods of improving the antistatic properties of synthetic fabric is to enhance the moisture regain. Increasing the moisture content of synthetic fiber improves its antistatic properties. In some works, water uptake has been improved by surfaced modification using plasmas.[4–7] In others, vinyl or acrylic monomer has been grafted onto the nylon to enhance its water absorption.[8] Mixing with chitosan can simultaneously improve the uptake of water as well as its antistatic properties.[9]

Many polymers including polyurethanes, polyurea, polyester, polyimide, and polyamide was cooperated with poly(ethylene oxide) (PEO) to improve their moisture regain.[10] Those block copolymers enable to be used in a wide range of applications, such as thermoplastic shape memory,[11] gas-sensing materials,[12,13] nanofibers formation,[14] and surface modification of cellulous film.[15] PEO is used as a compatible agent for LDPE/PA 6 blending.[16] A soft segment of PEO is introduced into nylon-6 to form a copolymer with improved toughness.[17–19] PEO provides flexible segments and hydrophilic moieties, which enable the nylon-6/PEO fiber to perform like a natural fiber,[20] making it an important constituent of biodegradable material by chain hydrolysis.[21] However, investigations of the basic properties of nylon-6/PEO copolymer and fiber, including their rheology, thermal properties, crystalline structure, and physical properties, are very few.

In this study, a series of PEO-based nylon-6 copolymers with various poly(ethylene oxide) diamine

Correspondence to: S.-P. Rwei (f10714@ntut.edu.tw).
Contract grant sponsor: National Science Council of the Republic of China, Taiwan; contract grant number: NSC-98-2221-E-027-004-MY3.

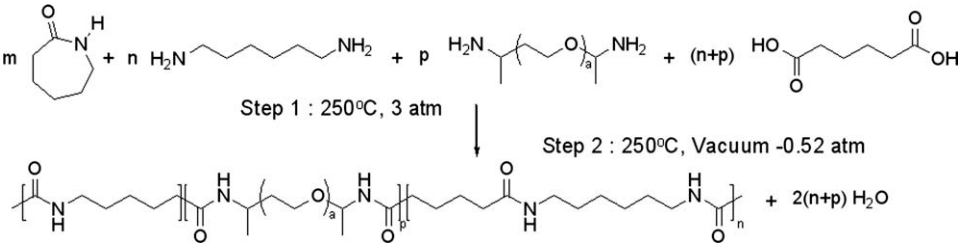

Scheme 1 Synthesis of nylon-6/PEO copolymers.

(PEODA) content were synthesized. Notably, two of the prepared batches were added hexamethylenediamine (HMDA) and adipic acid (AA) around 2 mol % into the PEO-based copolymers. All of the prepared copolymers were tested to determine their rheology using a capillary rheometer. The molar mass was examined by performing basic analyses such as relative viscosity (RV), gel permeation chromatograph (GPC), and amino-end group analysis. The thermal properties were investigated by differential scanning calorimetry (DSC). The crystalline structure of the copolymers (sheet) and fibers was examined by wide-angle X-ray diffraction (WAXD). More investigations of the fibers, examining the moisture regain and electric conductivity was carried following fabric formation. The maximum heat flux, q_{max}, which indicated a material warm/cooling feeling was also measured.[22–24] Finally, the electrical surface resistivity of the prepared fabrics was investigated to its antistatic property.

EXPERIMENTAL

Material

Caprolactam (CPL, >99.9%) was purchased from DSM. PEODA (>99%) was obtained from Huntsman, and its molar mass was about 2000. Adipic acid (>99.9%) was supplied by BASF. HMDA (Technical grade, 70% and remainder water 30%) was provided by Aldrich. The flake caprolactam, PEODA, stoichiometric adipic acid, and a small amount of water were charged into the autoclave (300 L).

Polymerization

The hydrolytic polymerization in a batch was used to obtain the nylon-6 and its copolymers. Three equilibrium reactions (ring opening, poly-addition, and poly-condensation) were involved in the hydrolytic polymerization simultaneously. High water content is favored to ring opening of CPL, but restrict the molar mass growth. Two-stage (pressure and vacuum) cycle was therefore introduced herein. The hydrolysis and addition reactions took place at the first stage where the pressure was maintained and water was held. The second step, a poly-condensation stage, carried on when the reactor was switched to a vacuum condition to suck the water out.

The reactor was purged by nitrogen several times before heating to ensure that it contained no residual oxygen. The temperature was raised to 250°C. To initiate the hydrolytic polymerization of CPL, the pressure was set to 3 atm to prevent the water from evaporating in the reactor, in which the ring opening reaction was quarantined. After 3 h, the pressure was slowly released to atmosphere pressure, evaporating the water. The vacuum system was started to maintain the pressure at about −0.52 atm. Scheme 1 describes the chemical reaction that then occurred. The molar mass was accelerated under the vacuum condition, and the desired molar mass was reached after 2 or 3 h. The molten copolymer was then cooled and pelletized. Some waste would be inevitably produced during pelletization for each batch. The pellets were immersed in hot water for 20 h to extract the unreacted caprolactam and oligomer, which were around 10% by weight in total. After washing procedure, the pellets were dried at 110°C for 20 h and stored in a special package to ensure no leakage.

Table I presents al of the constituents of the copolymers. It also records the amount of feeding raw materials (kg mole) and the yield of the resulted copolymers.

The feed ratio is PEO content to the amount of copolymer before extraction. The theoretical ratio is the PEO content to the amount of copolymer after extraction. Equations (1) and (2) show how they are related. (A is the feeding weight of the CPL; B is the feeding weight of PEODA; C is the feeding weight of HMDA; D is the feeding weight of AA).

$$\text{Feed ratio} = \frac{B}{A + B + C + D} \tag{1}$$

$$\frac{\text{Theoretical}}{\text{final ratio}} = \frac{B}{A \times 0.9 + B + C + D} \tag{2}$$

A small amount of water was produced from HMDA and AA, and it was neglected in our calculation. The synthesized neat nylon-6, and 2, 4, 6, 8, 10, 15, and 20 wt % PEO-based copolymers were

TABLE I
Formulation of Prepared Copolymers

Symbol	Content wt % PEO	Content Nyon-66 mol %	CPL kg	CPL kg mol	PEODA kg	PEODA kg mol	HMDA kg	HMDA kg mol	AA kg	AA kg mol	Waterl kg	PEO content before extraction (feed ratio %)	PEO content after extraction (Theoretical final ratio %)	The yield of the resulted copolymers (kg)[a]
P-0	0	0	100	0.885	0	0	0	0	0	0	4	0	0	70.2
P-2	2	0	96	0.850	1.77	0.00088	0	0	0.129	0.00088	4	1.81	2	67.6
P-4	4	0	92	0.814	3.46	0.00173	0	0	0.253	0.00173	4	3.61	4	65.3
P-6	6	0	88	0.779	5.08	0.00254	0	0	0.371	0.00254	4	5.44	6	62.5
P-8	8	0	84	0.743	6.62	0.00331	0	0	0.483	0.00331	4	7.27	8	60.9
P-10	10	0	80	0.708	8.07	0.00403	0	0	0.589	0.00403	4	9.10	10	57.0
P-15	15	0	63	0.558	10.1	0.00505	0	0	0.737	0.00505	4	13.68	15	38.3
P-20	20	0	54	0.478	12.4	0.00620	0	0	0.905	0.00620	4	18.42	20	31.6
P-A-6	6	2	88	0.779	5.25	0.00263	1.64	0.01414	2.45	0.01678	4[b]	5.39	6	65.3
P-A-8	8	2	84	0.743	6.85	0.00343	1.6	0.01379	2.51	0.01719	4[c]	7.21	8	62.5

[a] The yield of the resulted copolymers = the amount of feeding raw materials – the residual waste from polymer palletizing – the oligomer (CPL around 70 %) from extractive process.
[b,c] P-A-6 and P-A-8: The amount of water = the feeding water + the remainder water from HMDA solution.

denoted as P-0, P-2, P-4, P-6, P-8, P-10, P-15, and P-20, respectively. To two of the prepared batches of 6 wt % and 8 wt % PEO-based copolymers were added 2 mol % nylon-66, to form copolymers P-A-6 and P-A-8.

Measuring capillary flow

The apparent melt viscosities at various shear rates were measured by a capillary rheometer with a length/diameter ratio of 10 (GOTTFERT RHEO-GRAPH 25) at 270°C. The shear rate was adjusted from 10^3 to 10^4 s^{-1}.

Characterization

^{1}H-NMR was carried out using Bruker Avance DRX400 at 400 MHz to identify the chemical structure. Deuterated trifluoro acetic acid was used as a solvent. The reference compound was 100 mg Cholac/mL deuterated chloroform ($CDCL_3$) + 0.5% tetramethylsilane (TMS).

Determining molar mass

The molar mass of the prepared copolymers was estimated using three approaches.

Relative viscosity

The first approach was to measure relative viscosity (RV). The concentration of nylon-6 in sulfuric acid (96%) is 1 g/dL. RV was measured using Ubbelohde viscometer, which is a capillary viscometer, operated at a constant temperature 25°C.

Gel permeation chromatography

Gel permeation chromatography (GPC) analyses performed herein were on GPC/V2000 of Waters. The well-characterized narrow poly(methyl methacrylate) (PMMA) in hexafluoroisopropanol (HFIP) was used as the calibration standard. The various molar mass of PMMA was tabulated in Table II.

Amino end group analysis

The third approach was amino end group analysis.[25,26] About 0.5 g of the sample was placed in a 100-mL titration cup, and 50 mL of phenol/methanol mixture was added. The titration cup was stirred until the sample had completely dissolved. The solution was titrated with 0.01 *N* standard $HClO_4$. The blank, 50 mL of a mixture solvent, was titrated in the same way. The concentration of amino end groups was calculated in eq. (3). (*A* represents the volume of $HClO_4$, used as the solution and is given

TABLE II
Various Molar Mass of PMMA for GPC Calibration

Symbol	Molar mass	Retention time (min)
1	608,000	7.033
2	390,000	7.351
3	155,000	8.212
4	110,000	8.620
5	36,000	9.846
6	10,900	10.711
7	4,900	11.130
8	2,140	11.485
9	1,210	11.697

in mL; B is the volume of $HClO_4$ used as blank, given in mL; N is the equivalent concentration of the $HClO_4$, in eq/L, and W is the mass of the sample, in g.)

$$[-NH_2]\ \text{meq/kg} = \frac{(A - B) \times N \times 1000}{W} \quad (3)$$

Thermal properties

The thermal properties of the copolymers were measured by differential scanning calorimetry (DSC) using a TA Q-100. The heating rate was a controlled at 10°C/min from room temperature to 300°C and the latter temperature was held for 5 min to eliminate the thermal history; then and the copolymers were cooled at a constant rate of 10°C/min to 30°C.

Sheets prepared

All copolymer sheets were obtained by compression mold at 230°C. To prevent oxidation occurring during the cooling process, the cooling rate using cooling water system was accelerated immediately after the sheets formed.

Spinning yarn

POY

Two sets of godet were used and only 2 doffs were used in the winder. In this study, the designed spinnerets had 24 holes and the fibers were POYs. The specification of the filaments was approximately 70 den/24 f. The draw ratio was adjusted within the range 1.8–2.0 between the first and second godet. The speed of the first set of godet was set to around 1800 m/min, and the temperature was set 60°C. The corresponding parameter for the second godet was approximately 3400 m/min and 130°C, respectively. The pressure of interlace was maintained about 1.5 kg/cm^2. Eventually, the speed of winder was reach around 3200 m/min. at which it was maintained. The parameters, including draw ratio, take-up speed and throughput were then slightly adjusted according to each the characteristics of each batch of copolymer during the spinning process.

DTY

The DTY process was implemented, and the specification of the textured yarn was around 60 den/24 f. The POY was drawn and false-twisted using Teijin HTS-1500 type. The degree of drawing was determined by adjusting the speed of the draw roller, which ran faster than the feed rollers. The draw ratio and the disk/yarn speed ratio were nearly 1.2 and 1.8, respectively. The winder speed was maintained at 700 m/min.

Fabrics

DTY was applied to the fabrics, which were manufactured by knitting facility (Lawson-Hemphill Pineville Nc 28143). The specification of the circular knitted fabrics was 32 G.

Mechanical properties of fiber

The tenacity and elongation properties of the fibers were obtained at a constant rate of extension using Textechno (FPAC; No 35032). The mechanical properties of the fibers were measured using a gauge length of 500 mm, and the rate of extension was maintained about 600 m/min. The cycle time to rupture was around 20 s.

Boiling water shrinkage test

The POYs and DTYs were put for a few seconds in a container that was full of hot water. The yarns became shorter. The boiling water shrinkage (BWS) was obtained using eq. (4):

$$\text{Shrinkage}\ (\%) = \frac{(L_0 - L_1)}{L_0} \times 100 \quad (4)$$

Where L_0 was the yarn length before treatment with hot water, and L_1 was the length thereafter.

Wide-angle X-ray diffraction

Wide-angle X-ray diffraction was carried out at room temperature. The X-ray was generated from Cu Kα radiation ($\lambda = 0.154$ nm) at 45 kV and 40 mA using a Panalytical X'Pert Pro (MRD) PW3040/60. The scanning 2θ angle was from 10 to 60°.

Moisture regain

The absorption of moisture by the prepared circular knitting fabrics depends on ambient temperature

and relative humility (RH). The fabrics were maintained under two sets of conditions, which were 25°C, RH of 65% and 34°C, RH of 90%. Each prepared fabric weighed approximately 10 g. The moisture regain (MR) was obtained using eq. (5):

$$\text{Moisture Regain} = \frac{B - A}{A} \quad (5)$$

Where A is the mass of the dried sample before moisture treatment, and B is the mass of the sample after moisture treatment.

q_{max}

The maximum heat flux, q_{max}, indicates whether something feels instantaneously of warm/cool, and it is measured in W/cm^2. The q_{max} was examined using a KES-F Thermo Labo II.[27] The heat transfer per unit area was measured at a temperature difference of 10°C.

Surface resistivity of fabrics

The electric resistance of fabrics under specific conditions of RH and temperature was measured between two electrodes (according to AATCC 76). The specimens were maintained under two specific conditions. The first was an RH of 40% and a temperature of 20°C; the second was with an RH of 90% and a temperature of 34°C. Both conditions were maintained for 24 h, and then the static charge was measured.

RESULTS AND DISCUSSION

Polymerization

The yield was maintained about 60–70%. The weight loss was mainly from the extraction and pelletization. Detailed information associated with the yield was provided in Table I. The pellets produced herein had a diameter, length, and width of 2.3 mm, 2.5 mm, and 2.3 mm, respectively. All pellets were dried to less than 0.1 wt % (water content). The identification of the PEO content and the investigations of the physical properties were described in the later sections.

Measuring capillary flow

The melt viscosity of the copolymers decreased as the shear rate increased. The copolymers and the neat nylon-6 exhibited shear-thinning behaviors. Figure 1 plots the apparent viscosities of various compositions at 270°C. The melt viscosity at a PEO content of less than 10 wt % differed insignificantly from that of the neat nylon-6. However, viscosity considerably declined as the PEO content of the copolymer was increased to 15 wt %, probably because of the plasticizing effect of the PEO soft segments, and the consequent increases in the mobility of the molecular chain in the copolymers. Another reason was the intermolecular force between PEO and nylon-6 was weaker than that within nylon-6. Moreover, the viscosity of the copolymer with 20 wt % PEO could not be determined at high shear rate; thus, we eliminated P-15 and P-20 copolymers for spinning. The viscosities of the P-A-6 and P-A-8 copolymers were lower than that of neat nylon-6 and other copolymers. We posit that the low viscosity of P-A-6 and P-A-8 copolymers was a result of their low molar mass. The phenomenon reflects the results of the end group analysis on Table III. However, the apparent viscosity of both copolymers exceeds 30 Pa s at 10^4 s^{-1}; therefore, they both satisfied the requirement for spinning.

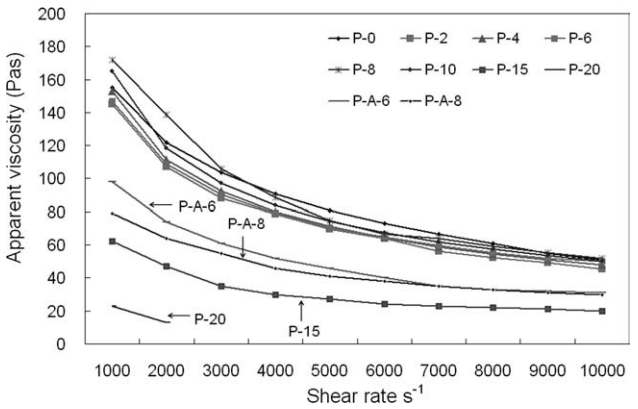

Figure 1 Apparent viscosity versus non-Newtonian shear rate at 270°C.

^{1}H-NMR spectra

^{1}H-NMR spectra were obtained to characterize the major segments of PEO and the nylon-6 backbone. The ^{1}H-NMR spectra of nylon-6 includes a typical chemical shift of less than 3.6 ppm. The PEO protons are easily recognized because they resonate at 3.9 ppm.[28] Figure 2 identifies the peaks of the PEO-based nylon-6 copolymer. The integration values of the proper signals were marked on the ^{1}H-NMR spectra. The superficial measurements of chemical shift at 3.9 ppm and others were well proportion to the PEO content in the copolymers. The experimental results were consistent with the theoretical ratio.

Determining molar mass

In this study, RV was utilized instead of intrinsic viscosity (IV) to compare the molecular sizes of prepared copolymers. Nylon-6 is a polar polymer, and sulfuric acid is a polar solvent. Therefore, P-0 had

TABLE III
Molar Mass Characterization by RV, GPC, and Amino End Group Analysis

Symbol	RV	M_n from GPC[a]	M_w from GPC[b]	PDI[c]	Amino-end group	M_n from end group analysis
P-0	2.7	25,103	54,809	2.18	52	19,231
P-2	2.5	49,033	104,321	2.13	55	18,182
P-4	2.19	45,700	99,628	2.18	49	20,408
P-6	1.86	54,399	115,446	2.12	48	20,833
P-8	1.83	45,742	99,817	2.18	45	22,220
P-10	1.8	43,321	96,150	2.22	42	23,809
P-A-6	2.17	43,934	95,902	2.18	63	15,873
P-A-8	2.04	43,444	95,977	2.21	58	17,241

[a] M_n, Number-average molecular weight.
[b] M_w, Weight-average molecular weight.
[c] PDI (polydispersity) = M_w/M_n.

an RV of around 2.7. PEO, however, is non-polar, so the expansion of the chain in sulfuric acid solution is suppressed. The RV of the copolymer decreased as the PEO content increasing. As expected, incorporating 10 wt % PEO into the nylon-6 reduced its RV dropped markedly from 2.7 to 1.8. The PEO-based nylon-6 copolymers with 2 mol % nylon-66 yielded very different results. When 2 mol % nylon-66 was added to 6 wt % and 8 wt % PEO-based copolymers, P-A-6 and P-A-8, their RV values increased from 1.86 and 1.83 to 2.17 and 2.04, respectively, revealing that adding a small amount of nylon-66 to copolymer increased its solubility in sulfuric acid.

GPC is an alternative way to estimate the molar mass. The nylon-6 dissolves in HFIP, forming the different hydrodynamic radius by polymer expanding in the solution. The GPC data of nylon-6/PEO copolymers exhibited almost twice the molar mass as that of pure nylon-6. The number average molecular weight (M_n) for P-0, P-2, and P-A-6 were 25,103, 49,033, and 43,934, respectively. Notably, the results from RV and GPC reveal a reverse trend, mainly due to the different solvent characters between HFIP and sulfuric acid. The sulfuric acid used in RV test is good for nylon-6, but poor for PEO. On the contrary, HFIP used in GPC test favors to PEO and results in the expanded conformation of the nylon-6/PEO copolymers. Figure 3 displays the PMMA calibration plot and the profiles of copolymers. The various molar mass of PMMA for calibration was corresponded to Table II. Neither bimodal nor multimodal was presented in Figure 3.

To obtain accurately the molecular size, amino end group analysis was carried out. Equation (6) yields the average molecular size.

$$\text{Number average molar mass} = \frac{1}{[-NH_2]\ \text{meq/kg}} \times 10^6 \quad (6)$$

The average molar mass of the copolymers were approximately 20,000, independently of PEO content. The results prove that the molar mass of these copolymers exceeded the critical value, 16,000, indicating that the synthesized copolymers were sufficiently large to form entanglements and to exhibit stable physical properties, as does neat nylon-6. Table III summarizes the results of the RV, GPC, and amino end group analyses of the prepared copolymers.

Thermal properties

Figure 4(a) plots the melting temperature (T_m) of the copolymers, determined from DSC measurements. The results indicate that the transition temperatures varied insignificantly deviation as the PEO content increase to 6 wt %. Incorporating a small amount of PEO into nylon-6 backbone did not disturb the original crystal lattice of the neat nylon-6. Flexibility and lack of bulkiness of the PEO chain are well known. PEO is reasonably assumed to have been squeezed into the amorphous phase, owing to its flexibility. Accordingly, the crystallinity of the nylon-6 was maintained. T_m did not significantly change as the PEO content was increased. Mateva et al.[17] also discovered that the T_m of nylon-6/polyisoprene did not apparently vary with polyisoprene content up to 10 wt %. They proposed that polyisoprene segments are located in the amorphous region. The results of our study, however, demonstrate a decrease in melting temperature as PEO content increased to 8 wt %, indicating that the inclusion of PEO-reduced crystallinity in the copolymers. However, the incorporation of the PEO decreases the heat of crystallinity while increasing the PEO content. At 8 wt % PEO copolymer, the T_m and the enthalpy of fusion were 219.4°C and 50.7 J/g, respectively. These values were around 1.8°C and the 7.1 J/g lower, respectively, than those of neat nylon-6. Furthermore, the crystalline peak became broader with increasing PEO content, suggesting that the PEO segments either reduced the degree of crystallinity or altered the crystalline

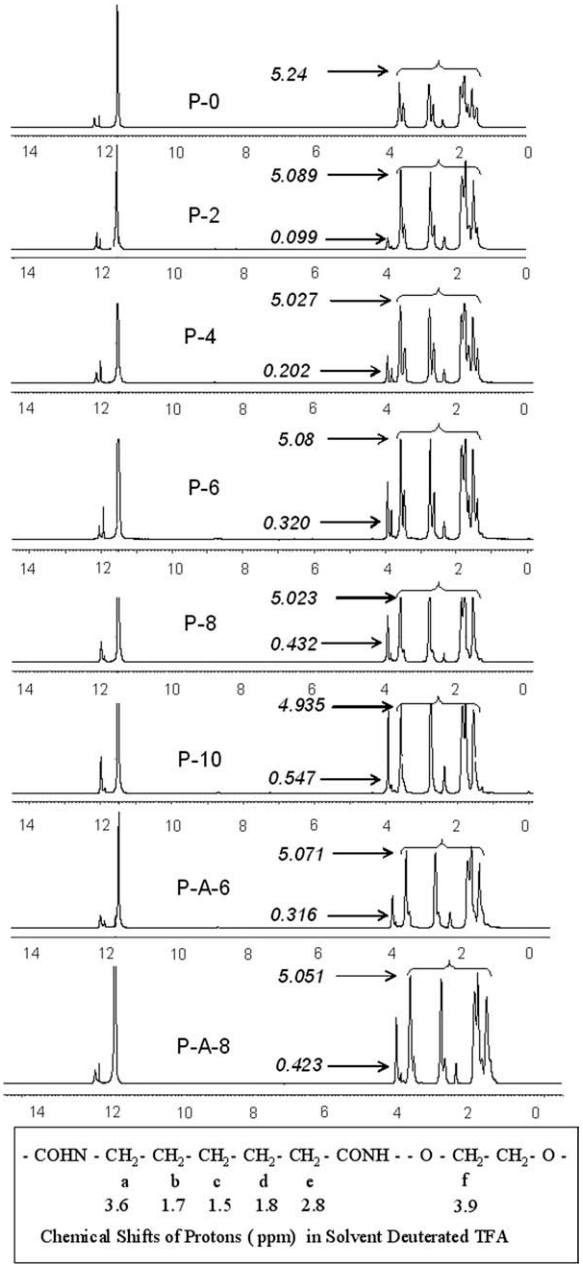

Figure 2 ^{1}H-NMR spectra of prepared copolymers.

phase. In contrast, the T_m reduced remarkably when 2 mol % nylon-66 was incorporated into the copolymers. —CH_2— from the structures of AA and HMDA, distributed randomly in the copolymer, caused defects in the packed crystalline lattices. Consequently, the melting point of P-A-6 and P-A-8 copolymers was 6–8°C lower than that of PEO-based copolymer. The cooling DSC scans in Figure 4(b) yield similar results. The crystalline temperature (T_c) did not significantly shift until to 8 wt % PEO has been incorporated. The T_c of the prepared copolymers exhibited the same phenomenon like the T_m. Introducing nylon-66 into the nylon-6 backbone decreased the T_c by around 6–8°C. Table IV summarizes the thermal properties of the prepared copolymers.

Properties of fibers

Mechanical test

The prepared copolymer fibers were synthesized by melt-spinning. Table V summarizes the tensile properties of POYs (before false-twist treatment) and DTYs (following false-twist treatment) that were formed from all of the prepared copolymers. Apparently, they were all less strength than neat nylon-6 (P-0) fiber. The plasticizing effect of PEO reduced both the intermolecular force and the degree of crystallinity in fibers, reducing the tensile strength. In particular, both P-A-6 and P-A-8 had a remarkably low tensile strength, corresponding to the low molar mass in Table III (amino end group analysis). In general, DTY had higher tenacity than POY due to enhancement of chain orientation. Table V showed the equilibrium and even slightly lower value of DTY's tenacity than that of POY's. The breakage of polymer chain during DTY process is the main reason because of high degree orientation of POYs. Another possibility is assumed that a slip-tilting of lamellae during DTY process, the splitting of the original crystal lattice into small blocks, resulting in a low tensile strength of the DTYs.[29] However, all results exceeded 4.5 g/den, indicating that the fibers satisfied the requirements of fabric.

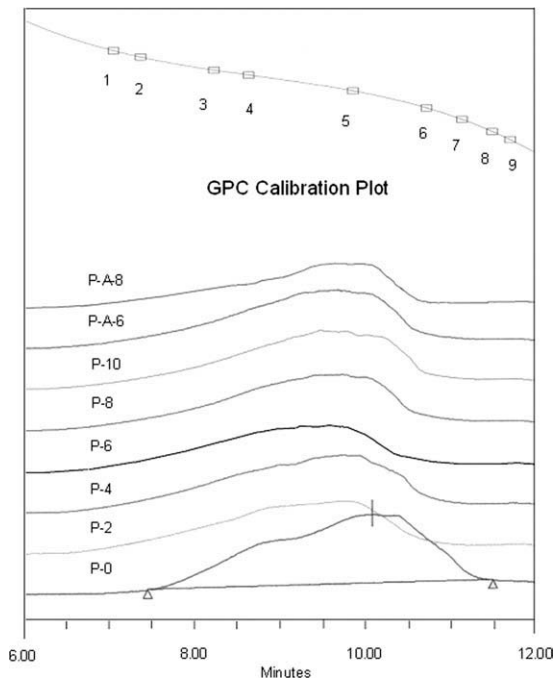

Figure 3 The GPC profiles for prepared copolymers. The various molar mass of PMMA for calibration was corresponded to Table II.

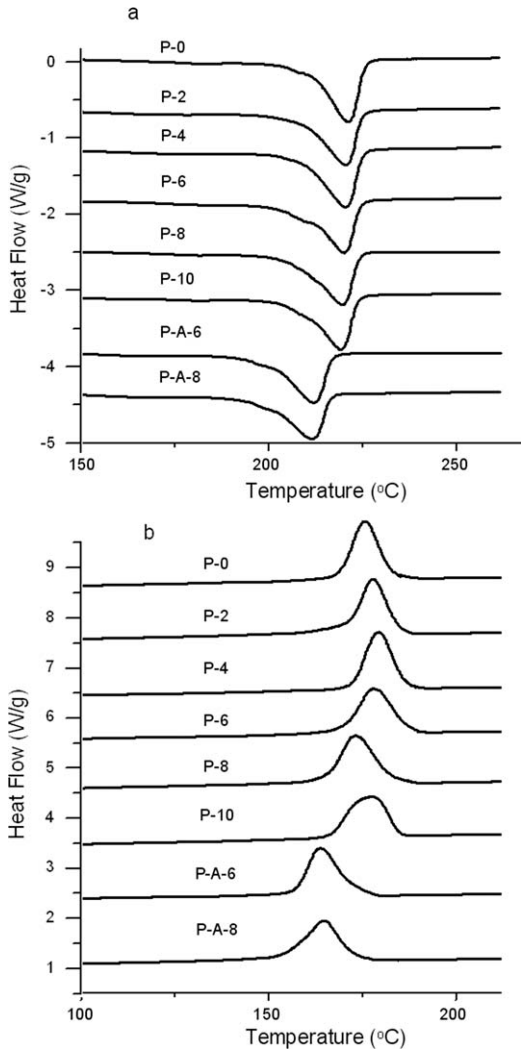

Figure 4 DSC scan curve of the prepared copolymers. (a) DSC curve for detecting the melting temperature. (b) DSC cooling scan curve for determining the cold crystallization.

Boiling water shrinkage test

The BWS of fibers is important to determining their potential use in textile. Figure 5 demonstrates that the BWS of fibers increased with PEO content. P-0 POY exhibits shrinkage of approximately 9.1%.

TABLE IV
Thermal Properties of Prepared Copolymers

Symbol	The melting temperature (°C)	ΔHm (J/g)	The crystallization temperature (°C)	ΔHc (J/g)
P-0	221.2	57.8	175.7	56.5
P-2	220.6	55.3	177.3	53.4
P-4	220.7	51.2	178.4	48.6
P-6	220.2	51.4	177.6	49
P-8	219.4	50.7	174.7	49.6
P-10	219.4	49	177.6	48.4
P-A-6	214.4	48.5	163.7	46.3
P-A-8	212.8	48.9	164.5	46.4

TABLE V
Tensile Properties of Fibers

	Specification (den)		Tenacity (g/den)		Elongation (%)	
Symbol	POY	DTY	POY	DTY	POY	DTY
P-0	67	60.6	5.32	5.61	73.6	32.8
P-2	69.5	59.7	5.27	5.41	66.8	33.1
P-4	70.1	59.9	4.97	5.19	66.9	35.8
P-6	69	61.8	5.26	5.05	64.8	26.2
P-8	70.8	61	4.95	5.09	64.3	27.3
P-10	70.8	61.7	5.15	4.85	60.2	36.8
P-A-6	70.9	62.4	4.52	4.87	70.1	22.7
P-A-8	70.8	60.3	4.63	5.08	62.3	34.7

Shrinkage changes considerably as the PEO content increases over 6 wt %. The BWS values of P-8 and P-10 were around 3.9 and 6.2%, respectively, higher than that of P-0 fiber. The BWS behavior is associated with the relation of internal stress by the extended noncrystalline molecular chains tend to more coiled conformation. Placing the fibers in boiling water can provide kinetic energy that can overcome the intermolecular forces. Consequently, the molecular length approaches that of the random coil conformation, as results of entropy. The increased in the BWS with PEO content is assumed to be caused by the drop in the crystallinity and decrease in the intermolecular forces among adjacent chains. When the fiber is immersed in hot water, the water penetrates the amorphous phase. Water interacts with amide, and new associations between N—H and H—O—H will be established, favoring the mobility of polymer segments.[30] Another probable cause is the ease mobility of PEO was easily extended in amorphous phase by orienting upon spinning. The extended chain of PEO more easily coiled back than the nylon-6 backbone. DTYs exhibit similar behavior. Notably, the BWS of DTY was higher than POYs. Gupta et al.[31] propose that the crystallinity and orientation simultaneously increase upon drawing. For nylon-6, the orientation effect is stronger than crystallinity. Therefore, the shrinkage of DTY was higher than POY for all prepared fibers.

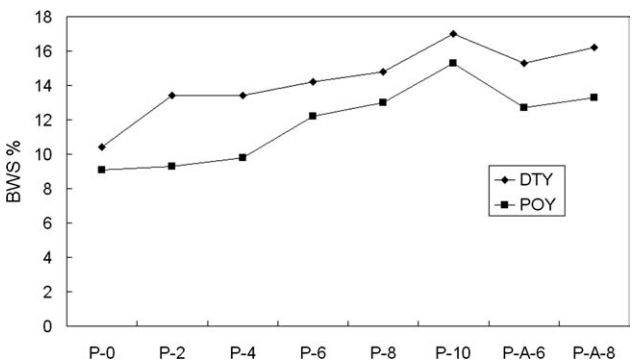

Figure 5 BWS curves of POYs and DTYs.

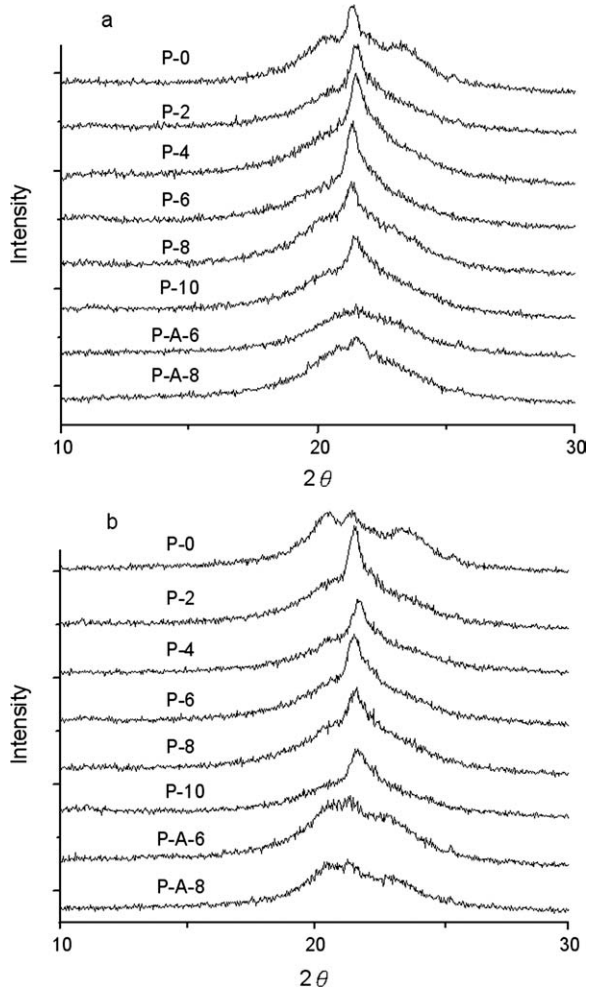

Figure 6 WAXS patterns of sheets. (a) Specimens before heat treatment. (b) Specimens after heat treatment.

WAXD

Pattern of sheets

WAXD experiments were carried out neat nylon-6 and its copolymers to determine their crystal structures. Three dominant diffraction peaks were obtained from P-0 [Fig. 6(a)]. The two at $2\theta = 20.5°$ and $2\theta = 23.5°$ are associated with the α-crystalline phase. The other diffraction peak at $2\theta = 21.5°$ is associated with the γ-crystalline phase. The dominant crystalline structure in P-2, P-4, P-6, P-8, and P-10 was dramatically converted from α to γ when PEO was incorporated into the copolymers. These results suggest that PEO disfavored the α form but favored the γ form of the crystal. The α-crystalline form of nylon-6 is reportedly associated with hydrogen bonds between adjacent antiparallel chains.[32] Therefore, the α-form is converted into the γ form by breaking partial H-bonds between adjacent sheets of nylon-6. The molecular chains in nylon-6 are linked together by hydrogen bonds between C═O and N—H groups, which contribute to the intermolecular force. Once PEO enters the backbone of nylon-6, the interactions between N—H and the ether groups (C—O—C) will alter the intermolecular structure. Haitao et al.[9] also indicated that the strong interaction between chitosan and nylon molecule causes new H-bonds to be formed. Yiping Qiu et al.[5] demonstrated that the moisture content significant affects the modifying effects of plasma treatment at atmospheric pressure. The original H-bonds are broken as water replaces the N—H groups. A. Etxeberria proposed that the number of hydrogen bonds between the carbonyl and N—H groups declined as the poly (ether amide) (PEA) content in the nylon-6/PEA composition.[33] Evidently, the original hydrogen bonds were broken as a consequence of the bonding of PEO with N—H group. The intermolecular hydrogen bonds were shifted from the pair of C═O and N—H to the pair of C—O—C and N—H. Adding PEO disturbed the formation of the intersheet hydrogen bonds in the crystalline structure, yielding a dominant γ form. The patterns of P-A-6 and P-A-8 are much broader than those of other copolymer sheets [Fig. 6(a)]. The nylon-66 contributed to the random structure of copolymer, not only by reducing the size of the crystal domain, but also by reducing the degree of crystallinity.

In verify the interaction between amide and ether groups, all specimens were heat-treated. The sheets were placed in a dryer, and maintained at 165°C under vacuum conditions. The annealing process lasted for three hours, before a second series of WAXD experiments were performed. Figure 6(b) shows the results. The patterns of all of the sheets revealed insignificant changes upon heat treatment. The γ form of the nylon-6/PEO copolymers did not observably transform to the α form upon heat treatment. Comparing the diffraction peaks before and heat treatment further proved that the original hydrogen bond between the pair C═O and N—H was replaced by that between the pair C—O—C and N—H. Consequently, no α crystal form of the P-2, P-4, P-6, P-8, and P-10 was obtained despite annealing. However, unexpected diffraction peaks from P-A-6, P-A-8 revealed that the γ form were converted to the α form after heat treatment when a small amount of nylon-66 was incorporated into the copolymers. However, the intensities of the α forms of P-A-6 and P-A-8 were much lower than that of P-0. The copolymers that comprised nylon-66 parts formed a new stable crystalline state. Thus, the structure of the copolymers was converted to the α form.[32]

Pattern of fibers

The pattern of POY of P-0 fiber revealed dominant γ forms, as did those of the P-2 and P-4 fibers. Figure 7(a) presents the disappearance of the γ form in

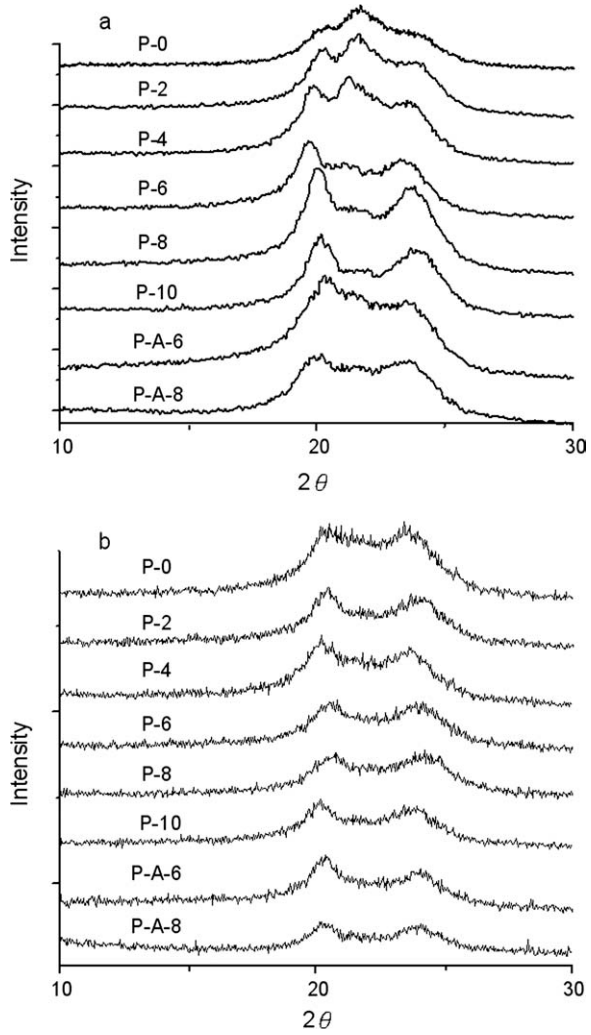

Figure 7 WAXS patterns of fibers. (a) POYs and (b) DTYs.

specific copolymers which the PEO wt% exceeded 6 wt %. Compared with sheets, the patterns for POYs show reverse results. Heuvel and Huisman[34] found the crystal in fibers is already generated completely, while the winding speed is higher than 3000 m/min. The γ phase is orientation-induced. When the velocity of the winder is high, strong orientation transforms the crystalline form to γ form. In this experiment, the winding speed was maintained at approximately 3200 m/min; therefore, the crystallization of POY of P-0 predominantly crystallize as the γ form, consistent with Heuvel's conclusion. However, the intensity of the signal from the γ forms of P-2 to P-4 fibers is weaker than that of P-0, and the α phase was formed simultaneously. The signal at $2\theta = 21.5^\circ$ from the γ forms is absent when the PEO content is exceeds 6 wt % (P-6 to P-10) and just the α form dominates the crystal structure. The finding differs dramatically from the result obtained for the sheets. The rate of crystallization of the nylon-6/PEO copolymer was believed to be lower than that of neat nylon-6 fiber; the crystallization did not proceed to completion during spinning despite the high winding speed. Hence, crystallization occurred on the bobbin. At this moment, the copolymer fibers were saturated with water and PEO segments, increasing the mobility of the molecular chain in the fibers. Many molecular chains in the noncrystalline domain were maintained in highly tensile state. The crystal phase was thus approached the stable α form; the dominant phase was converted from the γ form to the α form. The behavior also explained the PEO segments interrupted the oriented arrangement of the copolymer; therefore, the structure disfavored the formation of the γ phase during the single-axial draw process. A higher PEO content corresponded to a closer approach to the more stable α form upon fiber formation. Again, the signal of the α form of the copolymers with the 2 mol % nylon-66 (P-A-6 and P-A-8) was weak. Figure 7(b) presents the WAXD patterns of the prepared modified nylon-6 DTY. Apparently, all results present only one phase, the α form. The prepared POY flat yarns were transformed into crimped yarns using the draw textured facility. The POYs were drawn and false-twist-textured. The process again affected the crystal structure. During texturing, the fibers were deformed by bending or twisting. The original γ forms were destroyed by bending or twisting. Consequently, the crystalline structure was completely converted to α form.[35]

Moisture regains

Figure 8 presents that the absorption of water increased with the amount of PEO in the fabrics. PEO exhibits an important hydrophilic property, which significantly increasing the MR of the prepared fabrics. Introducing 10 wt % PEO into nylon-6 increased its MR value from 4.29 to 4.97 at 20°C and an RH of 65% and from 6.9 to 9.81 at 34°C and an RH of 90%. High-moisture fabrics like cotton are comfortable upon contact with human skin. At

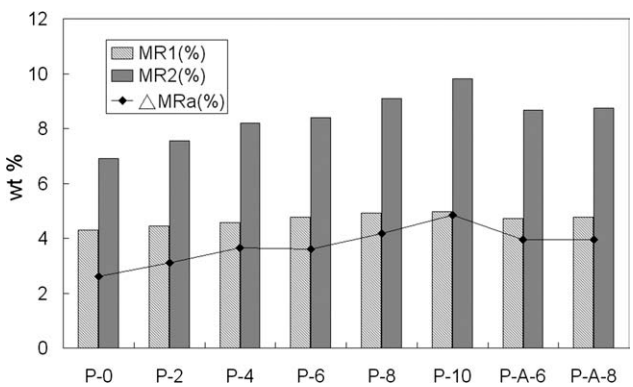

Figure 8 Moisture regain of the fabrics.

temperature of 34°C and an RH of 90% were used to simulate human skin; a temperature of 25°C and an RH of 65% were used in a simulation of the ambient atmosphere. The difference (ΔMR) between the MRs of the skin and ambient has a particular meaning: it captures the moisture transfer property as the rate of conduction of perspiration. According to Fick's law, a high ΔMR indicates a high rate of transport of perspiration from the body skin to the ambient. Figure 8 shows the MR and ΔMR of the fabrics both increased with PEO content. The ΔMR of the fabrics was improved from 2.6 to 4.8 when 10 wt % PEO was introduced into the nylon-6 backbone. In this investigation, the copolymers that contained nylon-66 had lower crystallinity, but an insignificantly raising higher MR value. At 34°C and an RH of 90%, the MR values for P-6 and P-A-6 were 8.39 wt% and 8.67 wt %, respectively. A similar difference was obtained for P-8 and P-A-8.

Index of warm/cool feeling, q_{max}

The q_{max} value (W/cm^2) indicates the instantaneous warm/cool feeling when the skin touches the fabric. A higher q_{max} indicates a more rapid transfer of heat from the body to the fabric. People feel cool when they touch the fabric. The identification of this characteristic has opened a new field of "cool fiber" application. Figure 9 demonstrates that q_{max} increased in proportion of PEO content. The q_{max} of P-10 was enhanced from 0.74 to 1.15 W/cm^2. High moisture content favors heat transfer. In a previous section, the fact that the MR was enhanced by increasing PEO content was discussed. Increasing PEO content significantly increases the moisture of the fabrics because PEO is hydrophilic. Therefore, the modified fabrics had a higher q_{max} than neat nylon-6. The q_{max} results agree closely with the behavior elucidated in the study of moisture regain.

Surface resistivity

The tendency of a fabric to accumulate electrical charge depends on its electrical resistance. More

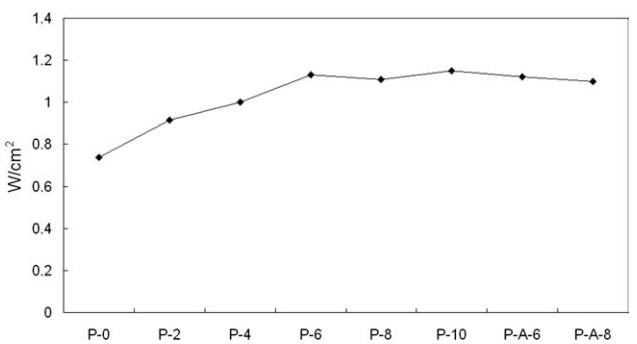

Figure 9 q_{max} of the fabrics.

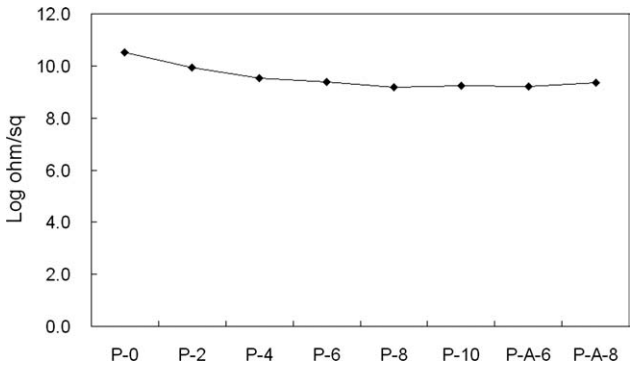

Figure 10 Surface resistivity of the fabrics.

charges accumulate on the surface of a fabric with higher resistivity. Nylon-6 has a low electric conductivity, causing some difficulty with processing and limiting its range of applications. In this study, the electric resistivity of fabrics was measured under two conditions. Under the first condition of RH = 40% at 20°C, the surface resistivity of all fabrics exceeded 10^{12} Ω/cm^2. Under the second condition of RH = 90% at 34°C, the surface resistivity of fabrics gradually declined as the PEO content increased. This change in surface resistivity was dominated by the increase in moisture content of the fabrics. At an RH of 40% and a temperature of 20°C, all of the treated fabrics had low moisture content, and therefore had a low electrical conductivity. At an RH of 90% and a temperature of 34°C, all of the treated fabrics had higher moisture content, and the electrostatic was dissipated through the water. Water promotes the electrostatic transport.[36] Consequently, fabrics with a higher PEO content had a surface resistivity that was approximately one order of magnitude lower than that of neat nylon-6. Figure 10 reveals that the surface resistivity of the fabric was improved from 3.26×10^{10} to 1.54×10^{9} Ω/sq when 8 wt % PEO was introduced into nylon-6. In this case, at an RH of 90% and a temperature of 34°C, the hydrophilic PEO segments enhanced the absorption of moisture, increasing the antistatic property of the fabrics.

CONCLUSION

A series of modified fibers, with PEO feed ratio of 0–10 wt % and 2 mol % nylon-66 were synthesized by condensation polymerization and pilot melting spinning. ^{1}H-NMR spectra verified the structure and the PEO content of each copolymer system. A rheological investigation indicated that neat nylon-6 and its copolymer behaved similarly at high shear rates when the PEO content was less than 10 wt %. With respect to thermal properties, determined by DSC, both T_m and T_c slightly declined as the PEO content in the copolymers increased. Once nylon-66 was

introduced into the polymer backbone, both T_m and T_c shifted markedly 6–8°C and the tensile strength were reduced below that of neat nylon-6 fiber. However, in all case, the tensile strength exceeded 4.5 g/den, indicating that the fibers satisfied the requirements of fabric. The BWS increased with PEO content. The WAXD results for sheets were the opposite of those for fibers. In sheet testing, adding a small amount of PEO to the copolymer altered its crystalline phase from α to γ, mainly by breaking some of the original H-bonds by the incorporation of ether groups. In POYs testing, the dramatically change from γ phase to α phase was assumed to the crystallization continued on the bobbin. The behavior was explained mostly by the interruption of the oriented copolymer arrangement by PEO segments; therefore, the structure disfavored to the formation of the γ phase upon single-axial draw process. The copolymer that contained nylon-66 exhibited α crystal phase in both sheet and fiber studies. The moisture regain increased significantly with the PEO content. However, nylon-66 in the copolymer apparently did not improve moisture regain herein. The modified fabrics had a higher q_{max} than neat nylon-6 because PEO is hydrophilic. The surface resistivity of fabrics at 34°C and an RH of 90% was improved by increasing the PEO content, also mostly because of an increase in water absorption.

We also thank Mr. Pao-Chi Chen and Mr. Ta-Yo Chen for help in polymerization and Miss. Hsiao-Wen Cheng for testing studies.

References

1. Jessica, A. H.; Julla, A. K.; Jeremiah, P. K. Adv Polym Technol 2004, 23, 135.
2. Krupa, I.; Mikova, G.; Novak I.; Janigova, I.; Nogellova , Z.; Lednicky, F.; Prokes, J. Eur Polym J 2007, 43, 2401.
3. Akif, K.; Saeed, S. N.; Richard, C. F. Synth Met 2008, 158, 1.
4. Daphne, P.; Andres, B.; Derek, J. D.; James, K.; Hirvonen, W. K.; Robert, J.; Steven, M. Surf Coat Technol 2006, 201, 4384.
5. Lu, Z.; Chunxia, W.; Yiping, Q. Surf Coat Technol 2007, 201, 7453.
6. Yan-Chun, L.; Yan, X.; Da-Nian, L. Appl Surf Sci 2006, 252, 2960.
7. Kartick, K. S.; Manjeet, J.; Ashwini, K. A. Surf Coat Technol 2009, 203, 1336
8. Chahira, M.; Stephane, M.; Sadok, R. Appl Surf Sci 2007, 253, 5521.
9. Haitao, Z.; Shubai, L.; Christopher, J. B. W.; Xin, N.; Huali, N.; Limin, Z. Electrochim Acta 2009, 54, 5739.
10. Anne, J.; Robert, C.; Pierre, L. Prog Polym Sci 2002, 27, 1803.
11. Qinghao, M.; Jinlian, H. Solar Energy Mater Solar Cells 2008, 92, 1245.
12. Jun, R. L.; Jia, R. X.; Ming, Q. Z. Min, Z. R.; Qiang, Z. Polymer 2005, 46, 11051.
13. Iwata, H.; Nakanoya, T.; Morohashi, H.; Chen, J.; Yamauchi, T.; Tsubokawa, N. Sens Actuators B 2006, 113, 875.
14. Hem, R. P.; Madhab, P. B.; Ki, T. N.; Kong, H. C.; Soo-Jin, P.; Hak, Y. K. Mater Lett 2010, 64, 2087.
15. Fusako, S.; Kaori, T.; Akio, K.; Yoichiro, M.; Mitsuru, A. J Appl Polym Sci 1999, 74, 1516
16. Asa, H.; Mehrnoush, J, D.; Bengt, W. Polymer 2001, 42, 8743.
17. Mateva, R.; Filyanova, R.; Dimitrov, R.; Velichkova, R. J Appl Polym Sci 2004, 91, 3251.
18. van der Schuur, M.; de Boer, J.; Gaymans, R. J. Polymer 2005, 46, 9243.
19. Hallden, A.; Deriss, M. J.; Wesslen, B. Polymer 2001, 42, 8743.
20. Lofquist, R. A.; Saunders, T. T. Y.; Twilley, I. C. Textile Res J 1985, 55, 325.
21. Bezemer, J. M.; Weme, P. O.; Grijpma, D. W.; Dijkstra, P. J.; van Blitterswijk, C. A.; Feijen, J. J Biomed Mater Res 2000, 52, 8.
22. Joanne, Y.; Kwong, C.; Kwan, M. S.; Kai, S. L. J Mater Process Technol 2002, 123, 5.
23. Tanaka, Y.; Sukigara, S. J Textile Eng 2008, 54, 75.
24. Kan, C. W.; Yuen, C. W. M. J Appl Polym Sci 2006, 102, 5958
25. Paul, C. H. Polymer Chemistry: The Basic Concepts; Marcel Dekker: New York, 1984
26. Joshi, H. D.; Joshi, D. H.; Patel, M. G.; Naik, S. R. Ind Text J 2008, 119, 29.
27. Johnson, S. J.; Mansdorf, S. Z. Performance of Protective Clothing, Vol.5.; ASTM Publication Code Number 04-012370-55 U.S.A
28. Silverstein, R. M.; Webster, F. X. Spectrometric Identification of Organic Compounds, 6th ed.; Hoboken, NJ: Wiley, 1997.
29. Tim, A. O.; Georg, M. Material Science of Polymers for Engineers; Hanser Publishers: Munich, 2003.
30. Anthony, A. Polyamide (Fibers). Kirk-Othmer Encyclopedia of Chemical Technology. Wiley, 2002.
31. Gupta, V. B.; Bashir, Z. Stoyko Fakirov. In Handbook of Thermoplastic Polyester, Vol.1; Fakirov, Z. S., Eds.; Wiley-VCH Verlag Gmbh: Weinheim, 2002
32. Melvin, I. K. Nylon Plastic Handbook; Hanser: New York, 1995
33. Etxeberria, A.; Guezala, S.; Iruin, J.; de la Campa, J.; de Abajo, J. Polymer 1998, 35, 1035
34. Heuvel, H. W.; Huisman, R. High Speed Fiber Spinning; Wiley-Interscience: New York, 1985
35. Gupta, V. B.; Kothari, V. K. Manufactured Fiber Technology; Chapman & Hall: London, 1997.
36. Bhat, N. V.; Benjamin, Y. N. Textile Res J 1999, 69, 38.